Shock Tube Pyrolysis of 1,2,4,5-Hexatetraene

Cheryl H. Miller, Weiyong Tang,† Robert S. Tranter,‡ and Kenneth Brezinsky*

Departments of Mechanical Engineering and Chemical Engineering, University of Illinois at Chicago, 842 West Taylor Street, M/C 251, Chicago, IL 60607

Received: October 19, 2005; In Final Form: January 11, 2006

1,2,4,5-Hexatetraene (1245HT) is, according to theory, a key intermediate to benzene from propargyl radicals in a variety of flames; however, it has only been experimentally observed once in previous studies of the $C_3H_3 + C_3H_3$ reaction. To determine if it is indeed an intermediate to benzene formation, 1245HT was synthesized, via a Grignard reaction, and pyrolysized in a single-pulse shock tube at two nominal pressures of 22 and 40 bar over a temperature range from 540 to 1180 K. At temperatures $T < 700$ K, 1245HT converts efficiently to 3,4-dimethylenecyclobutene (34DMCB) with a rate constant of $k = 10^{10.16} \times \exp(-23.4$ kcal/RT), which is in good agreement with the one calculated by Miller and Klippenstein. At higher temperatures, various C_6H_6 isomers were generated, which is consistent with theory and earlier experimental studies. Thus, the current work strongly supports the theory that 1245HT plays a bridging role in forming benzene from propargyl radicals. RRKM modeling of the current data set has also been carried out with the Miller−Klippenstein potential. It was found that the theory gives reasonably good predictions of the experimental observations of 1245HT, 1,5-hexadiyne (15HD), and 34DMCB in the current study and in our earlier studies of 15HD pyrolysis and propargyl recombination; however, there is considerable discrepancy between experiment and theory for the isomerization route of 1,2-hexadien-5-yne (12HD5Y) → 2-ethynyl-1,3-butadiene (2E13BD) → fulvene.

Introduction

The molecular growth of small aromatic species is purported to produce soot particles, therefore, the formation of the first aromatic ring, benzene or phenyl, is of particular interest. The recombination of propargyl radicals, R1,

$$C_3H_3 + C_3H_3 \rightarrow C_6H_6 \quad \text{(R1a)}$$

$$\rightarrow C_6H_5 + H \quad \text{(R1b)}$$

is widely thought to be a primary route to benzene and phenyl formation in a variety of aliphatic flames. Thus, a full understanding of R1 is vital in constructing accurate detailed aromatic mechanisms.[1−3]

The recombination of propargyl radicals forms three linear C_6H_6 compounds: head-to-head forms 1,5-hexadiyne (15HD), head-to-tail forms 1,2-hexadien-5-yne (12HD5Y), and tail-to-tail forms 1,2,4,5-hexatetraene (1245HT) (where the head is the CH_2 end and the tail is the CH end of propargyl). At suitable temperatures, these three linear species then isomerize to various secondary C_6H_6 isomers: *trans*-1,3-hexadiene-5-yne (*trans*-13HD5Y), *cis*-13HD5Y, 3,4-dimethylenecyclobutene (34DMCB), 2-ethynyl-1,3-butadiene (2E13BD), fulvene, benzene, and the phenyl radical.[4] Beginning with the pioneering work of Alkemade and Homann in 1989,[5] and particularly in the past few years, considerable progress has been made in understanding the mechanistic routes of R1.[6−17] In a flow reactor/mass spectrometry (MS) study, Alkemade and Homann detected 15HD, 1245HT, 12HD5Y, 13HD5Y, and benzene as the products of R1 at 623 and 673 K and 3 mbar and 6 mbar.[5] Fahr and Nayak detected 15HD and two unidentified C_6H_6 species (one of the species thought to be 12HD5Y) as products of R1 at 298 K and 50 torr.[6] Scherer et al. used a Poraplot-Q column in the GC (gas chromatography)/MS analysis of a residual gas sample of their shock tube experiments and observed eight C_6H_6 species, with two of them identified as benzene and 15HD.[7] In the laser photolysis/MS study by Schafir and co-workers,[8] 15HD, fulvene, benzene, and two unidentified C_6H_6 isomers were observed at 500−1000 K and 2−8 mbar. Howe and Fahr identified 15HD, 12HD5Y, 34DMCB, fulvene, and benzene as products at 20 and 700 Torr from 295 to 623 K.[9] More recently, our high-pressure single-pulse shock tube study of 15HD pyrolysis coupled with GC-mi-FTIR (gas chromatography-matrix isolation-FTIR spectroscopy) analyses led to the observation and identification of eight C_6H_6 products.[10,11] In our subsequent study of propargyl recombination, a small amount of 1245HT was also detected, and the initial branching ratios of R1 were experimentally determined.[12] In addition, several experimental studies have obtained the overall recombination rate constant of R1 over a wider temperature and pressure range.[13−17]

In terms of kinetic modeling of reaction R1, Miller and Klippenstein[4] calculated a potential energy surface diagram for the recombination of propargyl radicals; the reaction pathways for the recombination of propargyl radicals forming benzene and phenyl + H are illustrated in Figure 1. As clearly shown in Figure 1, 1245HT is one of the primary products of propargyl recombination, and there are two routes to benzene formation. In addition to the fulvene route, benzene is formed by *cis*-13HD5Y, which is formed via 1245HT. With the phenomenological rate coefficients obtained by RRKM master equation

* Corresponding author. E-mail: kenbrez@uic.edu.
† Current address: Gamma Technologies Inc., 601 Oakmont Ln, Westmont, IL 60559.
‡ Current address: Chemistry Division, Argonne National Laboratory, Argonne, IL 60439.

10.1021/jp055990v CCC: $33.50
Published on Web 02/22/2006

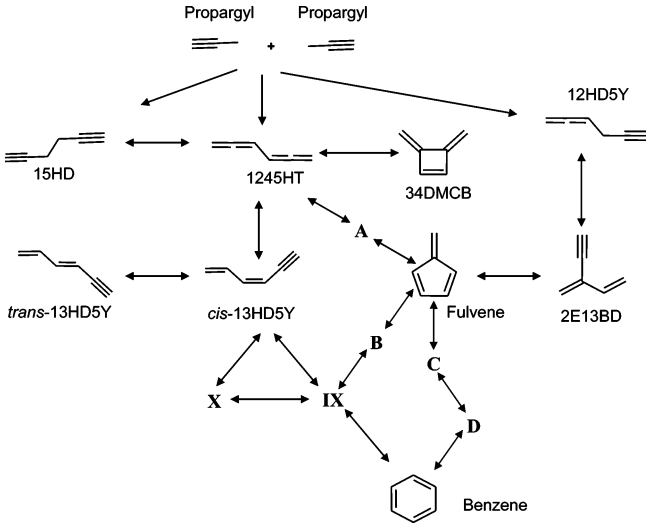

Figure 1. Chemical reaction pathway involving stable species of the recombination of propargyl radicals and subsequent C_6H_6 isomerization. The length of the arrow does not indicate the significance of the path. 15HD, 1,5-hexadiyne; 1245HT, 1,2,4,5-hexatetraene; 12HD5Y, 1,2-hexadiene-5-yne; 34DMCB, 3,4-dimethylenecyclobutene; 13HD5Y, 1,3-hexadiene-5-yne; 2E13BD, 2-ethynyl-1,3-butadiene. X, IX, A, B, C, and D are highly reactive intermediate C_6H_6. Refer to ref 4 for detailed energy levels and structures of X, IX, and A−D.

calculations, the Miller and Klippenstein potential is able to accurately predict the product yields of 15HD pyrolysis in an atmospheric flow reactor study at 250−550 °C by Stein and co-workers.[18] Kislov et al. [19] also calculated a C_6H_6 potential; however, it was not validated against available experimental data. In addition, there is an alternative approach proposed by Tang et al. [20] in modeling the $C_3H_3 + C_3H_3$ reaction by optimizing the rate coefficients against detailed experimental C_6H_6 isomer concentration profiles.

Even though the theoretical work of Miller and Klippenstein hypothesizes that 1245HT is a significant part of the propargyl recombination mechanism, there is only one experimental study, conducted by Alkemade and Homann,[5] in which 1245HT was identified as a major product. Thus, there is a discrepancy between experimental observations of propargyl recombination and the theoretical predictions for propargyl recombination. The present work studied the pyrolysis of 1245HT to determine if the isomerizations of 1245HT are consistent with the theoretical work of Miller and Klippenstein. RRKM analysis was also utilized to further evaluate the energetics of the Miller and Klippenstein potential.

Experimental Section

1. High-Pressure Single-Pulse Shock Tube. The pyrolysis experiments were performed in a high-pressure single-pulse shock tube. Since the shock tube has already been described in detail in refs 21 and 22, it is only described briefly in this paper. The shock tube operates routinely at temperatures up to 2000 K and pressures up to 1000 atm with reaction times of a few milliseconds. The major sections of the high-pressure single-pulse shock tube are the driver section (60 in. long, 1 in. bore reduced from the normal 2 in. for this work), the driven section (101 in. long 1inch bore), the high-pressure storage tanks, the dump tank, the diaphragm section, and the sampling rig. In each experiment, a shock wave is initiated by increasing the pressure in the driver section to rupture the diaphragm. Samples are then withdrawn into the sample rig from the volume close to the endwall of the driven section that has experienced the conditions behind the reflected shock wave.

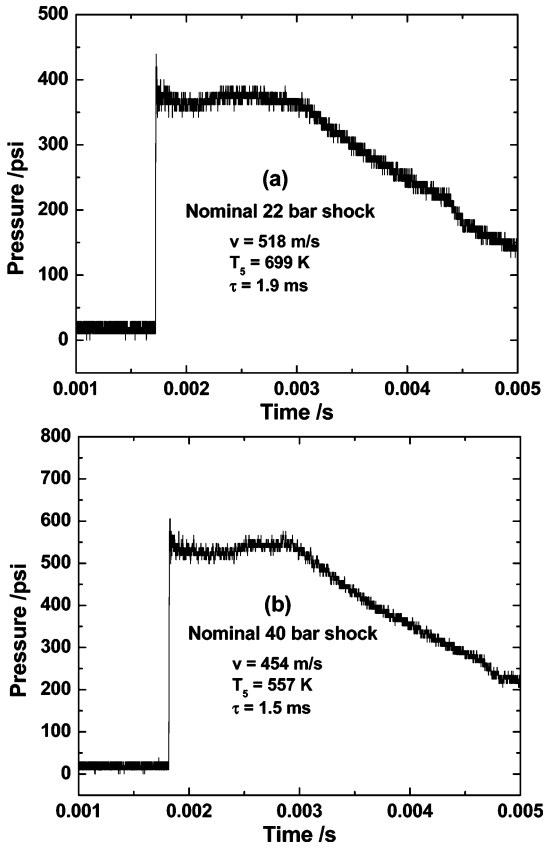

Figure 2. Typical low-temperature shock profiles at (a) 22 bar, 699 K, and (b) 40 bar, 557 K.

The techniques for measurement of the shock tube end wall reaction pressure, P_5, the reaction temperature, T_5, the residence time, and the sampling time, t, are similar to our previous work.[11,12] Briefly, pressures behind the reflected shock wave and reaction times were obtained from the pressure profiles measured by a piezoelectric pressure transducer (model no. PCB 113A23) mounted axially in the end wall of the driven section. The reaction time of each experiment was measured from the arrival of the incident shock wave at the end wall of the driven section to the observed pressure at the end wall falling to 80% of its maximum. The reaction temperatures were calculated from the incident shock velocity, and errors in the temperature due to deviations from ideal gas behavior were expected to be small. Shock velocities were calculated from the time taken for the incident shock wave to travel between piezoelectric pressure transducers mounted along the side wall of the driven section near the end of the shock tube. In the current work, the UIC HPST was modified to generate very low shock velocities in order to investigate the low-temperature decomposition of 1245HT while maintaining a decent "plateau" shock profile. This was achieved by reducing the driver section diameter to 1.0 in. i.d. from its usual value of 2.0 in. through the use of a reducer sleeve in the driver section. The use of a narrow bore driver (1.0 in. i.d.) would probably lead to a greater attenuation of the shock waves, as compared to the 2.0 in. i.d; however, this is accounted for by the way the shock velocities are measured and hence incorporated into the calculation of T_5 and P_5. In the current study, aluminum diaphragms of 0.025/0.010 in. (thickness/score depth) and 0.025/0.005 in. were employed, generating nominal end wall pressures of 22 and 40 bar, respectively. These diaphragms generate nominal 25- and 50-

bar end wall reaction pressures, respectively, in the unmodified shock tube configuration. As expected, the shock waves produced by the same sets of diaphragms are slightly weaker than in previous studies because the driver gas volume is reduced by the reduction in the driver section diameter. Two typical low-temperature shock profiles at nominal 22 and 40 bar are displayed in Figure 2a and b, respectively.

2. Synthesis of 1,2,4,5-Hexatetraene (1245HT). Because 1245HT was not available commercially, 1245HT was synthesized by a method developed by Hopf and co-workers.[23−26] The synthesis is essentially a Grignard reaction, which is a two-part process. The first part is the formation of the Grignard reagent, R2, and the second part is the reaction of the Grignard reagent with an electrophile to form a new carbon−carbon bond, R3. In the first part of the synthesis, allenyl-magnesium bromide, which is the Grignard reagent, is formed by reaction of magnesium turnings (Sigma Aldrich, ≥99.5%) and propargyl bromide (TCI America, >97%). In the second part of the synthesis, allenyl-magnesium bromide reacts with propargyl bromide in the presence of copper(I) chloride (Sigma Aldrich, >99.995%) as a catalyst to form 1245HT in addition to 12HD5Y, 34DMCB, and 15HD. Because the Grignard reagent reacts readily with water, oxygen, and carbon dioxide, diethyl ether (Fluka, ≥99.8%) was used as the solvent due to its volatility, and the synthesis was carried out in an inert atmosphere of nitrogen. The details of the synthesis are given in refs 25, 26. The synthesis product was then purified to discard a large amount of diethyl ether, first by normal distillation under atmospheric nitrogen and then by a vacuum distillation.

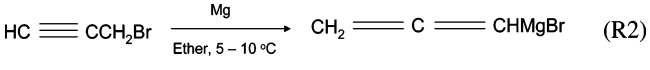

(R2)

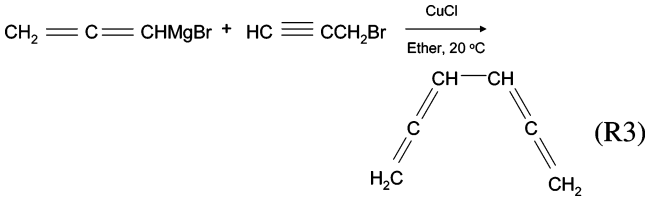

(R3)

The results of the synthesis were confirmed by gas chromatography-matrix isolation-FTIR spectroscopy-mass spectrometry (GC-mi-FTIR-MS), which allows simultaneous collection of FTIR and MS data. The total ion chromatogram (TIC) of the synthesis product sample is shown in Figure 3. In addition to 1245HT, a large amount of 12HD5Y and small quantities of 15HD and 34DMCB were also present in the product solution. The exact concentrations of each species varied from synthesis to synthesis, but a typical composition is 29% 1245HT, 4% 15HD, 17% 34 BMCB, and 50% 12HD5Y. The FTIR spectrum of 1245HT was identified based on the molecular structure and the expected results of the synthesis. This spectrum is nearly identical to the spectrum of 34MDCB with the exception of peaks at 850 and 1950 cm^{-1} in the 1245HT spectrum, as shown in Figure 4. In addition to the FTIR data, the retention times of 34DMCB and 1245HT on the GC column are very different, and the elution order of all the C_6H_6 species is the same as in the earlier work on 15HD isomerization. The reader is referred to our earlier publication[10] for the FTIR spectra and elution characteristics of the other C_6H_6 compounds.

Several methods have been attempted to isolate a purer form of 1245HT; however, they have not proved successful.

3. Preparation of Reagent Mixture. The reagent mixture was prepared manometrically in a 50-L tank. The reagent

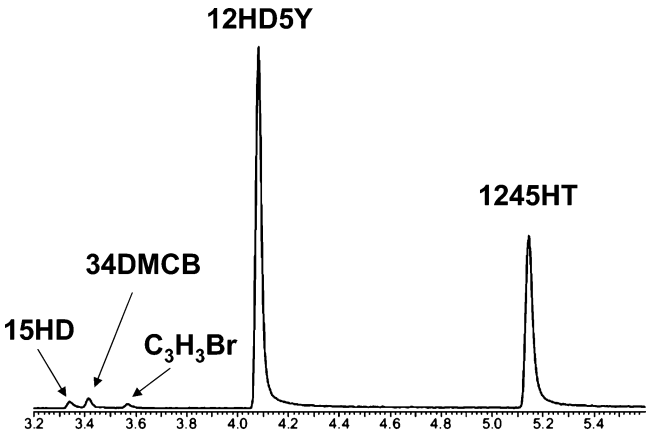

Figure 3. Total ion chromatograph (TIC) of the Grignard synthesis.

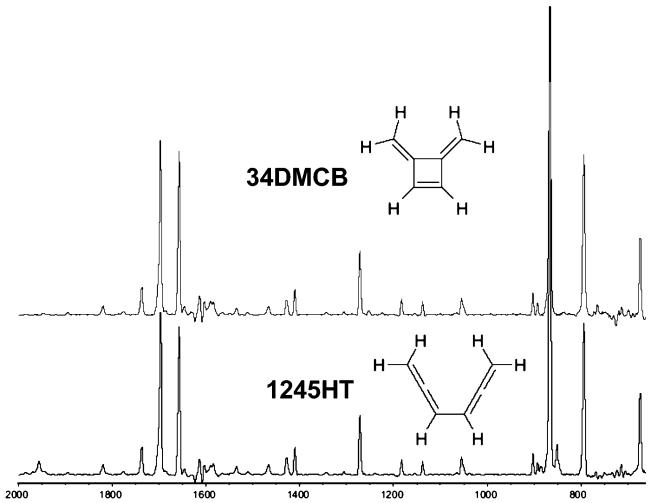

Figure 4. Comparison of the FTIR spectra of 1245HT and 34DMCB. (Note the differences of these two compounds at 850 and 1950 cm^{-1}.)

mixture was prepared a day in advance of the experiments in order to allow the reagent gases to mix by diffusion. The reagent mixture contained about 58.17 ppm of diethyl ether, 2.71 ppm of 15HD, 13.32 ppm of 34DMCB, 40.51 ppm of 12HD5Y, and 25.21 ppm of 1245HT in a bath gas of argon (BOC, 99.999% purity). The reagent mixture also contained about 200 ppm of neon (AGA, 99.99% purity) to correct for dilution effects if the driver gas-diluted the postshock sample. Even though the reagent mixture consisted of diethyl ether and C_6H_6 species other than 1245HT, the study of the pyrolysis of 1245HT was not altered or affected. As mentioned later in the Discussion section, the decomposition of diethyl ether is insignificant in the temperature range in which the isomerization of 1245HT occurs, and our earlier work on 15HD isomerization indicates that no radical species will be formed from the other C_6H_6 isomers at the reaction conditions of the current work.

4. Analytical Techniques. The routine analysis of the preshock and postshock samples was done by an Agilent 6890 series GC equipped with a flame ionization detector (FID) and a thermal conductivity detector (TCD). There were two columns in the GC, an HP-1MS column (30 m × 320 μm × 3 μm), which was connected to the FID, and an HP-PLOT Molsieve 5A column (30 m × 320 μm × 25 μm), which was connected to the TCD. The purpose of the TCD was to determine the concentration of neon, and the purpose of the FID was to determine the concentration of the stable hydrocarbons. The samples were injected into the GC by injecting the gas sample into two Valco gas sampling valves via a pressure reduction

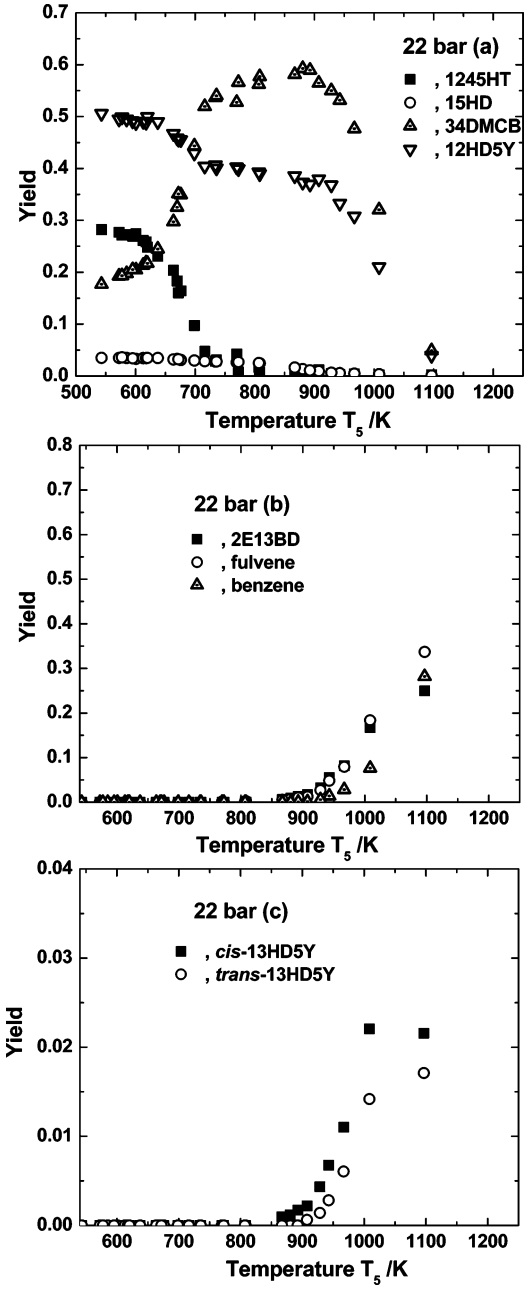

Figure 5. Isomeric product distributions at 22 bar.

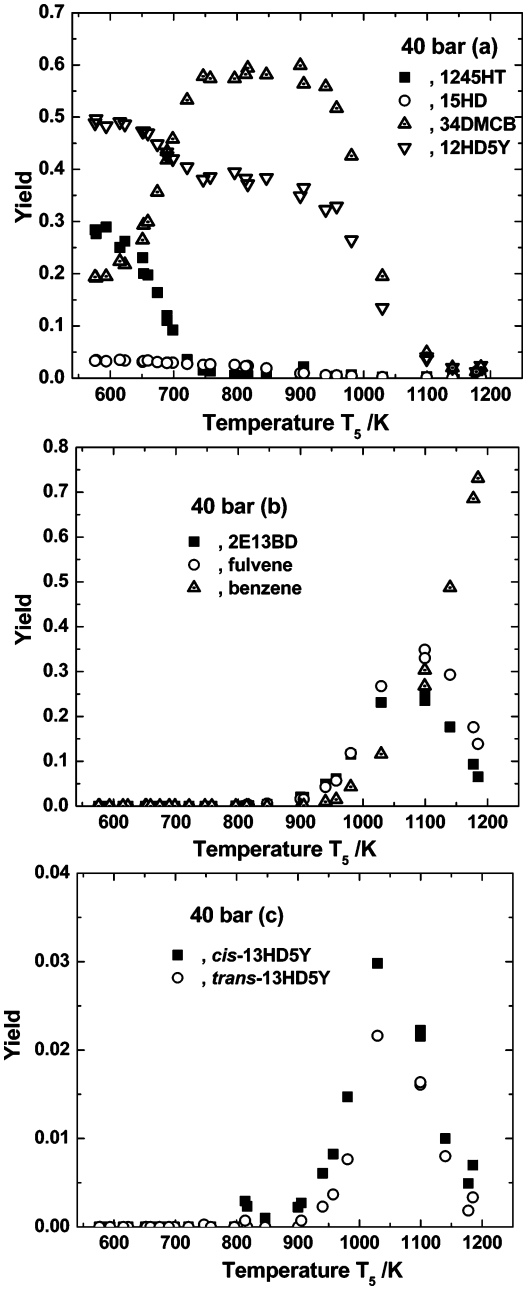

Figure 6. Isomeric product distributions at 40 bar.

vessel. The sample loops, which were connected to the two gas sampling valves, were filled simultaneously, and the sample entered the head of both columns simultaneously after the GC's valves were moved to the on position. In the initial stages of the experiments, an Agilent 6890 series GC coupled with an Agilent 5973 mass selective detector (MSD) was used to determine the molecular formulas of the species in the samples and the identities of certain species in the samples. This GC contained an HP-1 column (30 m $\times$ 320 μm $\times$ 3 μm), which was connected to the MSD.

Results

More than 60 experiments spanning a temperature range of 540−1180 K were carried out in order to map out the product distributions of the pyrolysis of 1245HT and 15HD5Y at two nominal pressures of 22 and 40 bar. The relative percentages of the C_6H_6 species in the reactant mixtures were 29% 1245HT, 4% 15HD, 17% 34DMCB, and 50% 12HD5Y.

The species concentration profiles with respect to temperature at postshock pressures of 22 and 40 bar are shown in Figures 5 and 6, respectively. The species concentration is represented by the concentration of the species in the postshock sample relative to the sum of the concentrations of the C_6H_6 species in the postshock sample. Figure 7 illustrates the pressure effects on 1245HT decomposition. As shown in Figure 7, the concentration of 1245HT is nearly identical for the 22- and 40-bar experiments. All of the other species behaved similarly, indicating all the chemistry is within the high-pressure limit in these experiments.

The initial reactants in the present work are 1245HT, 15HD, 12HD5Y, and 34DMCB. At about 600 K, 1245HT begins to decay and 34DMCB begins to increase as 15HD remains constant. 12HD5Y starts to decay at about 650 K and then remains constant between 715 and 900 K. 15HD starts to decay at about 780 K and is completely consumed by about 1000 K. Between 600 and 800 K, the 1245HT and 34DMCB appear to mirror each other. However, at around 800 K, the 1245HT is

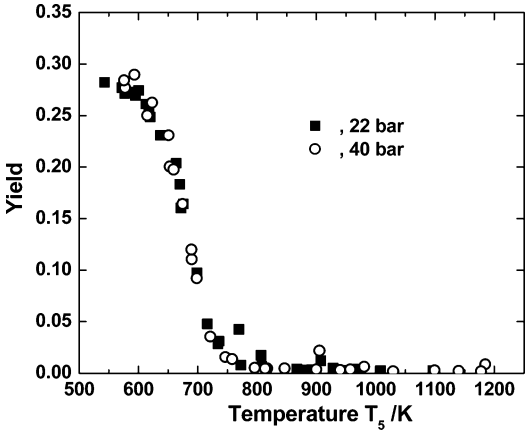

Figure 7. Effect of reaction pressure on the decomposition of 1245HT.

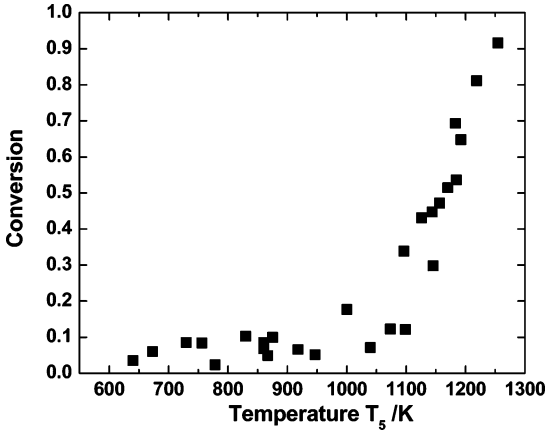

Figure 8. Shock tube pyrolysis of diethyl ether.

almost completely consumed and the 34DMCB concentration continues to increase at a slow rate to a maximum at around 900 K. In the 800−900 K interval, the 34DMCB and 12HD5Y profiles almost mirror each other. In the same interval, the 15HD is also converted to 34DMCB; however, the initial concentration of 15HD in these experiments is too low to account for the magnitude of the increase in 34DMCB.

On the basis of our earlier work,[11,12] it is safe to assume that, at temperatures less than 1100 K, the C_6H_6 isomers simply isomerize between the different forms. If 34DMCB is formed only from 1245HT and 15HD, then for temperatures <900 K,

$$[34DMCB]_{max} = [15HD]_0 + [1245HT]_0 + [34DMCB]_0$$

where subscript 0 refers to initial conditions and subscript max refers to the maximum concentration. For the experiments shown in Figures 5 and 6, the above expression is unbalanced, with about 0.1 more 34DMCB being formed than the expression predicts. This amount corresponds to the change in [12HD5Y] in the temperature range 650−900 K. Thus it would appear that, in this range, there is an isomerization between 12HD5Y and 34DMCB with possibly a slow back reaction as well.

Above 900 K, 34DMCB decays and fulvene starts to form along with benzene, *cis*-13HD5Y, and *trans*-13HD5Y, which appear at about 925 K. At about 900 K, 12HD5Y enters a steep decay and 2E13BD begins to form. The profiles of *cis*-13HD5Y and *trans*-13HD5Y are almost identical, except that the relative yield of the cis isomer is slightly greater than the relative yield of the trans structure. At about 1180 K, *cis*-13HD5Y and *trans*-13HD5Y are almost completely consumed. Above 1100 K, all of the remaining species except benzene are decaying.

In the current work, the carbon balance was monitored for each shock. The carbon balances show considerable scatter over the whole temperature range that cannot be attributed to the formation of heavy, nonvolatile species during the course of the reaction, and no wall deposits were observed in the shock tube. Currently, the source of the scatter is not clear, although it is potentially due to the GC rigs, the shock tube, and mixture tanks being unheated, which was necessary to prevent degradation of the reagent mixture, particularly 1245HT.

The experimental data sets, including reaction conditions and product distributions, are available in the Supporting Information.

Discussion

1. Decomposition of Diethyl Ether ($C_2H_5-O-C_2H_5$). Because diethyl ether was one of the components of the reagent mixture, shock tube studies of diethyl ether decomposition were performed in order to determine if diethyl ether is stable at the reaction conditions of the decomposition of 1245HT. The decay of diethyl ether has two competing channels of $CH_3CH_2O + C_2H_5$ and $C_2H_5OH + C_2H_4$.[27] Previously, Hohlein and Freeman investigated the radiation-sensitized pyrolysis of diethyl ether over 300−400 °C and observed the products ethane (C_2H_6), ethanol (C_2H_5OH), acetaldehyde (CH_3CHO), methane (CH_4), CO, ethylene (C_2H_4), and *n*-C_4H_{10}.[28] However, during the course of their work, the reactant experienced a temperature cycle of 30 min of heating and 30 min at the reaction temperature, and in the current work, the residence time of the shock tube is only 1.0−2.0 ms. Because of the short reaction times of the current study, diethyl ether most likely does not decay in the shock tube at the temperatures at which 1245HT starts to isomerize (∼600 K). As verification, in the present study, a reagent mixture consisting of approximately 115 ppm of diethyl ether and 200 ppm of neon (to correct for any dilution effects) in a bath gas of argon was prepared. The experiments were carried out at a nominal reaction pressure of 22 bar, reaction temperatures between 613 and 1254 K, and reaction times between 1.5 and 2.0 ms. The conversion of diethyl ether with respect to temperature is shown in Figure 8. Because there was no overall rate coefficient available in the literature, the current diethyl ether experiments were used to obtain, based on a first-order kinetics assumption, an overall rate coefficient for the decomposition of diethyl ether, R4. The derived rate coefficient is $k_4 = 10^{10.91} \exp(-43.34 \text{ kcal/RT})$, with a correlation coefficient of 0.91. The deduced activation energy is considerable lower than the previous work by Seres and Huhn, where a rate expression of $10^{17.19} \exp(-82.47 \text{ kcal/RT})$ for the dissociation reaction $C_2H_5-O-C_2H_5 \rightarrow CH_3CH_2O + C_2H_5$ at 697−761 K and 0.04−0.22 bar were derived from fitting to a complex mechanism. The prediction of the current expression is about one to two orders higher in the temperature range 900−1100 K at 22 and 40 bar.

$$C_2H_5-O-C_2H_5 \rightarrow \text{Products} \qquad \text{(R4)}$$

In the present work, the temperature region of most interest lies below 800 K, where the isomerization of 1245HT is complete, and clearly, at these temperatures, the effects from any decomposition of diethyl ether will be negligible. Additionally, no evidence has been found for the formation of products either from the decomposition of diethyl ether or from the reaction of ethyl radicals with C_6H_6 species at the reaction conditions of this study.

2. Product Analysis. Previous studies of the $C_3H_3 + C_3H_3$ reaction distinguished three possible initial pathways forming

15HD, 1245HT, and 12HD5Y through various head/tail combinations. When reaction conditions are favorable, the initially formed C_6H_6 complexes can dissociate into H atoms and phenyl radicals, but not at the low temperatures of our experiments. At our conditions, the preferred fate of the recombination products is either stabilization by collisions with the bath gas or thermal isomerization into various other isomeric C_6H_6 species, with benzene as the ultimate product. 12HD5Y can form benzene via 2E13BD and then fulvene, as shown in Figure 1. 15HD first isomerizes to 1245HT by a Cope rearrangement and then shares the same routes as 1245HT forming benzene. Unlike 12HD5Y, which apparently has only one benzene formation route, 15HD and 1245HT have an alterative route forming benzene via 13HD5Y without passing through fulvene, as proposed by Miller and Klippenstein. This alternative route was confirmed and was postulated to be the dominant route forming benzene at low temperature in our previous study of 15HD pyrolysis.[11]

In the current work, the relative yields of isomeric C_6H_6 products were found to be strongly temperature dependent, as anticipated, with 15HD, 12HD5Y, 34DMCB, 2E13BD, fulvene, and benzene as the major products and *cis*- and *trans*-13HD5Y as the minor products, which is consistent with our previous shock tube study of 15HD pyrolysis[11] and direct propargyl recombination.[12] At about $T = 600$ K, 1245HT starts to decay as 34DMCB increases, confirming that 1245HT forms 34DMCB because 15HD does not contribute to the formation of 34DMCB in this low temperature range. 1245HT is almost completely consumed at 720 K. This explains the results of our previous studies that 1245HT was not observed in the 15HD pyrolysis study in the temperature range between 780 and 1360 K and only a trace amount of 1245HT was detected in the propargyl recombination study between 720 and 750 K. After the consumption of 1245HT and 15HD, 34DMCB starts to decay, returning to 1245HT to form fulvene and *cis*-13HD5Y, which are the two routes to benzene formation. Benzene begins to form as *cis*-13HD5Y begins to form. After *cis*-13HD5Y is consumed, benzene continues to form, while fulvene begins to decay. Therefore, benzene is formed in parallel to fulvene at lower temperatures and sequentially to fulvene at higher temperatures. Eventually, all of the species isomerize to form benzene, the sole remaining species at high temperatures. In this regard, the present work supports the theoretical work of Miller and Klippenstein in which 1245HT is an essential bridging intermediate in the $C_3H_3 + C_3H_3$ reaction.

A point of interest and peculiarity is the concentration profile of 12HD5Y at low temperatures. 12HD5Y is one of the direct recombination products of propargyl radicals and was previously detected only in Alkemade and Homann's work and Fahr's work. However, these experiments did not observe 2E13BD, which is difficult to understand because, according to the Miller and Klippenstein potential, 12HD5Y can only be destroyed via 2E13BD. In the current work, 12HD5Y is constant at temperatures below 650 K and then starts to decay. It continues to decay until about 720 K and then remains constant until about 920 K. Then, it starts to decay again and form 2E13BD. In our earlier study of propargyl recombination in the temperature range of 720−1350 K,[12] the concentration profile of the initially formed 12HD5Y was found to be stable until 920 K. The profile of 12HD5Y in the earlier study is nearly identical to the profile of 12HD5Y in the present work. A plausible explanation of the behavior of 12HD5Y in the low-temperature regime is the isomerization of 12HD5Y to 34DMCB, a route that has not yet been included in current theory. This assumption requires further experimental study using pure 12HD5Y as the parent molecule and also further theoretical study.

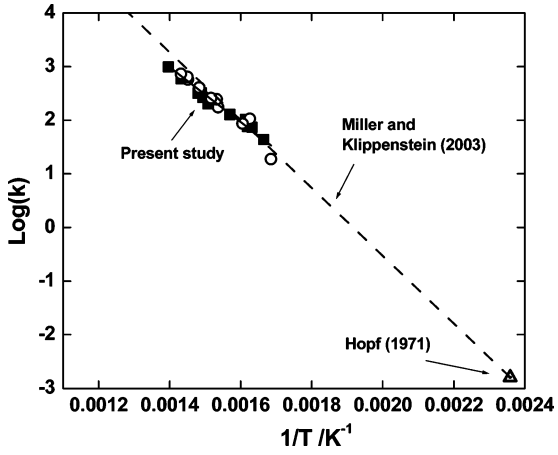

Figure 9. Comparison of the Arrhenius plots for the isomerization of 1245HT. The solid line is the least-squares fit using the current 1245HT pyrolysis data. Closed symbols: 22 bar data; open symbols: 40 bar data.

3. Rate Coefficient of the Decomposition of 1,2,4,5-Hexatetraene (1245HT). The results of the present work were used to evaluate a reaction rate coefficient for the decomposition of 1245HT to 34DMCB, R5, assuming that 34DMCB is the sole product. This fitted rate coefficient of $k_5 = 10^{10.16} \times \exp(-23.4 \text{ kcal/RT})$ is the first experimental Arrhenius rate coefficient expression for the decomposition of 1245HT. Figure 9 shows our measurements at 22 and 40 bar and the plot of a fitted Arrhenius expression from the measurements. Also, the predicted rate coefficients by Miller and Klippenstein are shown in this figure. In addition, the rate constant of a previous experimental study of 1245HT isomerization (1.16×10^{-3} s^{-1}) by Hopf [29] at 424 K and pressures of 35 and 60 Torr is shown in this figure. As Figure 9 illustrates, the rate coefficient of the present work is in good agreement with the previous calculated and measured rate coefficients of R5.

$$1245\text{HT} \rightarrow 34\text{DMCB} \qquad \text{(R5)}$$

4. RRKM Analysis. The most advanced, so far, potential energy surface for the $C_3H_3 + C_3H_3$ recombination reaction is the one proposed by Miller and Klippenstein, which was calculated by a combination of QCISD(T) and density functional (B3LYP) methods.[4] Their theoretical predictions have been qualitatively validated since all of the predicted C_6H_6 species from their surface have been identified in various experiments. By using their electronic calculation results, RRKM-based master equation (ME) analysis shows the theory is able to accurately predict the product yields of 15HD pyrolysis in a flow reactor by Stein and co-workers.[18] In the current work, Troe's modified strong collision (MSC) RRKM analysis was utilized to further test in a quantitative way the potential against shock tube measurements from the present study of 1245HT pyrolysis and from our earlier studies of 15HD pyrolysis and propargyl recombination.

The measured distributions of the species in the five early wells, namely 1245HT, 15HD, 34DMCB, 12HD5Y, and 2E13BD, served as modeling targets. The current study adopted two separate truncated kinetic models of Miller and Klippenstein for RRKM modeling. The current study used one of the models (referred to as model A) to simulate 15HD and 1245HT, which is shown in Table 1, and used the other model (referred to as model B) to simulate 12HD5Y, which is shown in Table 2. In

TABLE 1: Truncated Kinetic Model A used for RRKM Analysis of the Thermal Isomerization Initialized from 15HD and 1245HT[a]

reaction no.	reaction	barrier height/kcal
1	15HD → 1245HT	37.4[b]
2	1245HT → 15HD	40.9
3	1245HT → 34DMCB	29.6[c]
4	34DMCB → 1245HT	43.2
5	1245HT → A	39.1
6	A → 1245HT	19.1
7	1245HT → *cis*-13HD5Y	41.7
8	*cis*-13HD5Y → 1245HT	53.9
9	A → fulvene	71.5
10	fulvene → A	9.0
11	*cis*-3HD5Y → *trans*-13HD5Y	49.1
12	*trans*-13HD5Y → *cis*-13HD5Y	49.1

[a] Note: Critical energy values were taken from ref 4, A is an intermediate as in Figure 1. [b] Barrier height 35.4 kcal by electronic calculations and 36.4 kcal used for kinetic analysis in ref 4. [c] Barrier height 29.6 kcal by electronic calculations and 30.3 kcal used or kinetic analysis in ref 4.

TABLE 2: Truncated Kinetic Model B used for RRKM Analysis of the Thermal Isomerization Initialized from 12HD5Y[a]

reaction no.	reaction	barrier height/kcal
1	12HD5Y → 2E13BD	30.0
2	2E13BD → 12HD5Y	46.6
3	2E13BD → fulvene	55.6
4	fulvene → 2E13BD	86.7

[a] Note: Critical energy values were taken from ref 4.

both models, the reactions considered are only the initial thermal isomerizations from the chemically activated C_6H_6 adducts formed by the self-recombination of C_3H_3 radicals. The neglect of the dissociation reactions involving H-elimination should not cause significant errors under our temperatures. To avoid the complexity of including all intermediate C_6H_6 compounds, benzene was excluded from both models. Nevertheless, these two truncated models should be able to give reasonable representations of the Miller and Klippenstein potential in predicting the species formed in the early wells at moderate temperatures. In the RRKM-ME analysis by Miller and Klippenstein,[4] the 15HD → 1245HT and 1245HT → 34DMCB barrier heights were increased by 1.0 and 0.71 kcal/mol respectively over those calculated, to achieve good agreement with experimental observations. In the present work, we found it desirable to increase the 15HD → 1245HT barrier height by 2.0 kcal/mol over those by theory. No further adjustments were made.

The RRKM treatment of these two truncated kinetic models is as follows. All pressure-dependent rate constants were extracted by performing Troe's modified strong collision (MSC) RRKM calculations.[30−32] A RRKM program[33] previously developed only for single-well single-channel systems was extended for an arbitrary system with multiple wells and multiple channels. The RRKM parameters (ν_i, I_A, I_B, and I_C) for all individual activated complex and transitional states (TS) were all taken from the supplementary file of ref 4 by Miller and Klippenstein, without any alteration. An important consideration is the collisional efficiency of the argon diluents, which is a very weak collider for intermolecular energy transfer. We have used Troe's equation of

$$\frac{\beta_c}{1-\beta_c^{1/2}} = \frac{-\langle \Delta E \rangle_{All}}{F_E k_B T} \qquad (1)$$

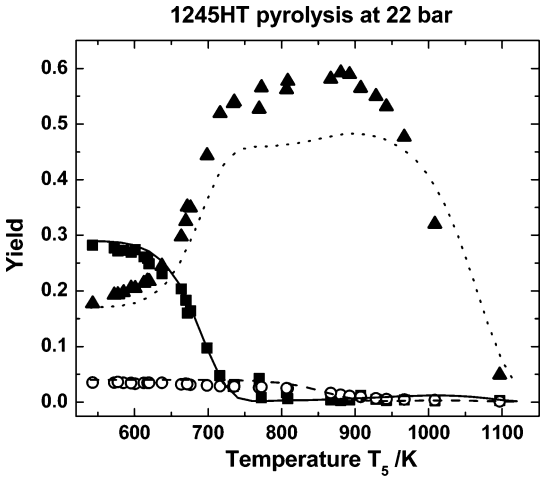

Figure 10. RRKM-ODE modeling of 1245HT pyrolysis at 22 bar. Initial reagent compositions were 29% 1245HT, 4% 15HD, 17% 34DMCB, and 50% 12HD5Y. Model A in Table 1 was used. Symbols represent the current experimental data and lines represent model predictions; ■ and solid line, 1245HT; ○ and dashed line, 15HD; ▲ and dotted line, 34DMCB.

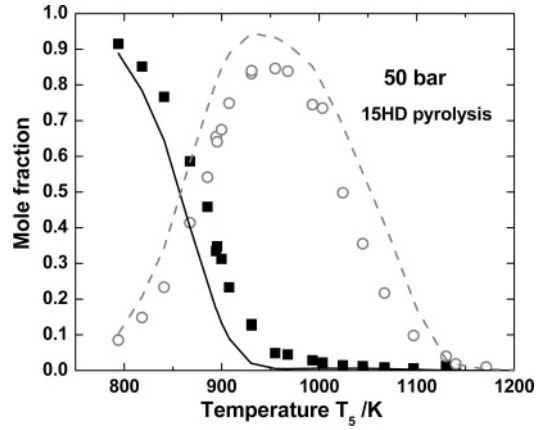

Figure 11. RRKM-ODE modeling of 15HD pyrolysis at 50 bar. The same kinetic model was used as in Figure 10. Symbols represent experimental data obtained from 1,5-hexadiyne pyrolysis (ref 11) and lines represent model predictions. The initial concentrations was $[15HD]_0 = 1.0$; ■ and solid line, 15HD; ○ and dashed line, 34DMCB.

to evaluate the collision efficiency, β_c. In eq 1, $\langle \Delta E \rangle_{All}$ is the total average energy transferred per collision and can be calculated from the downward average energy transferred per collision, $\langle \Delta E \rangle_{down}$, which was assumed to be 1000 cm^{-1} for all complexes and TSs. F_E is the energy dependence factor of the vibrational density of states and is calculated from

$$F_E = \frac{\int_{E_0}^{\infty} \rho(E) \exp(-E/k_B T)\, dE}{k_B T \rho(E_0) \exp(-E_0/k_B T)} \qquad (2)$$

To avoid possible errors induced in the procedure of fitting the RRKM calculated rate constant to an Arrhenius expression, the current RRKM program was linked directly to an ODE integrator DASAC.[34] Consequently, the RRKM calculation was performed at each temperature and pressure of interest, and the results of the RRKM calculation were used directly without extracting the traditional Arrhenius parameters. The predicted product yields were then plotted with the experimental measurements.

Figures 10−12 depict the RRKM-ODE modeling results of the 1245HT and 15HD entry channels by use of model A. It is

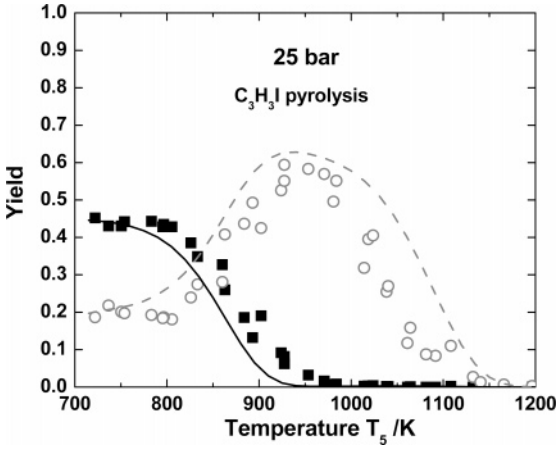

Figure 12. RRKM-ODE modeling of the $C_3H_3 + C_3H_3$ reaction at 25 bar. The same kinetic model was used as in Figure 10. Symbols represent experimental data obtained from C_3H_3I pyrolysis (ref 12) and lines represent model predictions. The initial concentrations were $[15HD]_0 = 0.44$ and $[1245HT]_0 = 0.18$; ■ and solid line, 15HD; ○ and dashed line, 34DMCB.

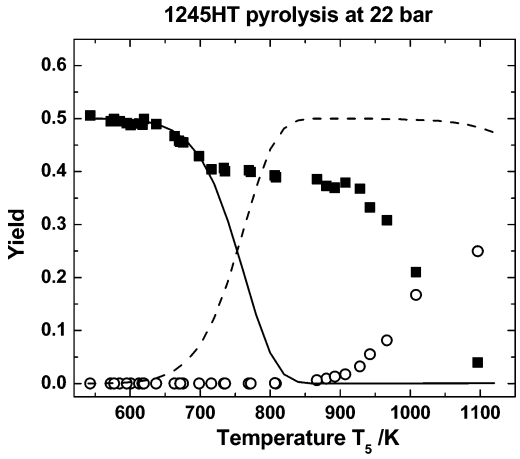

Figure 13. RRKM-ODE modeling of 1245HT pyrolysis at 22 bar. Initial reagent compositions were 29% 1245HT, 4% 15HD, 17% 34DMCB, and 50% 12HD5Y. Model B in Table 1 was used. Symbols represent the current experimental data and lines represent model predictions; ■ and solid line, 12HD5Y; ○ and dashed line, 2E13BD.

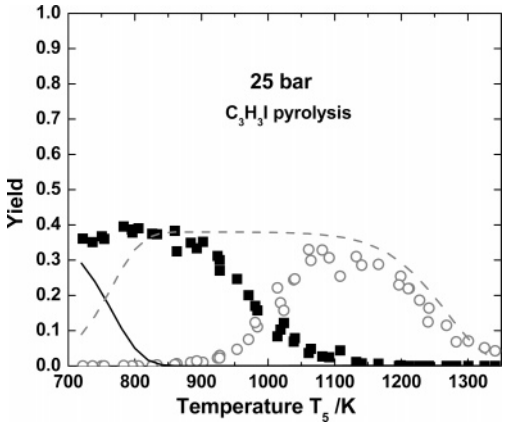

Figure 14. RRKM-ODE modeling of the $C_3H_3 + C_3H_3$ reaction at 25 bar. The same kinetic model was used as in Figure 13. Symbols represent experimental data obtained from C_3H_3I pyrolysis (ref 12) and lines represent model predictions. The initial concentrations was $[12HD5Y]_0 = 0.38$; ■ and solid line, 12HD5Y; ○ and dashed line, 2E13BD.

found that the result of the current RRKM-ODE modeling is predominately affected by the critical energy and the lowest vibrational frequencies. At our experimental pressures of 22 and 40 bar, most isomerization reactions are expected to be close to their high-pressure limits, and the simulation result does not show much sensitivity to the variation of downward transfer energy. The simulated product yields of 1245HT, 15HD, and 34DMCB in the 1245HT pyrolysis at 22 bar are shown in Figure 10. Figure 11 presents the predicted and measured 15HD and 34DMCB mole fractions for the 15HD pyrolysis at 50 bar, for which the simulation was conducted by using $[15HD]_0 = 1.0$. Figure 12 compares the model A predictions and the experimental observations of 15HD and 34DMCB in the recombination of propargyl radicals, for which the simulation was conducted by using the experimentally determined entry branching ratios as initial concentrations, with $[15HD]_0 = 0.44$ and $[1245HT]_0 = 0.18$.[12] Except in the 1245HT isomerization, where the peak 34DMCB concentration is underpredicted, the Miller and Klippenstein potential gives fairly good predictions of 1245HT, 15HD, and 34DMCB in all three experimental studies. 1245HT is predicted to be completely destroyed, with 34DMCB as the dominant product, even with the presence of 15HD, which is consistent with experimental observation. The underprediction of the 34DMCB is on the same order that the experimental $[34DMCB]_{max}$ is greater than $[15HD]_0 + [1245HT]_0 + [34DMCB]_0$.

The discrepancy between theory and experiment, however, becomes pronounced, as shown in Figures 13 and 14 in simulating the 12HD5Y channel, by use of model B. The theory is able to simulate the lower temperature 12HD5Y rearrangement to 2E13BD in the current data set but fails at higher temperatures, as shown in Figure 13. This is also shown in Figure 14, where the model indicates a quite efficient decay of 12HD5Y, clearly because of the low barrier height of 30.0 kcal for 12HD5Y → 2E13BD. The predicted 12HD5Y is consumed almost completely at 820 K, but at this point, the observed isomerization is still barely starting. In the $C_3H_3 + C_3H_3$ potential calculated by Miller and Klippenstein, 2E13BD is the sole isomerization product, via a five-member-ring transitional state. The considerable gap between theory and experiment in the depletion route of 12HD5Y → 2E13BD → fulvene suggests the necessity of reevaluation of the C_6H_6 potential. To fit the experimental data, either the barrier height of 12HD5Y to 2E13BD is significantly reduced or an additional route is added in current potential to form 12HD5Y at 800−1000 K.

Conclusions

The pyrolysis of 1245HT was studied at two nominal pressures, 22 and 40 bar, and at a temperature range of 540−1180 K in a single-pulse high-pressure shock tube. The analysis of the products demonstrated that the isomerizations of 1245HT are consistent with the theoretical work of Miller and Klippenstein [4] and the experimental work of Tranter et al.[11] and Tang et al.,[12] which was the first and foremost objective of this work. The current work further supports the notion that 1245HT is a significant part in the propargyl recombination mechanism. In addition, an experimental Arrhenius rate coefficient expression for the decomposition of 1245HT to 34DMCB was derived for the first time. This rate coefficient is in excellent agreement with the previous theoretical rate coefficient of Miller and Klippenstein and the single-temperature rate constant from the experimental work of Hopf. By using Troe's MSC/RRKM analysis, it was found that the current theory is generally capable of predicting the experimental observations in the current study and in our earlier work of 15HD pyrolysis and propargyl

recombination. However, the theory is not able to give a reasonable description of the depletion of the 12HD5Y channel. The current work strongly indicates that, at low temperatures, there is an apprant isomerization between 12HD5Y and 34DMCB that predominantly removes 12HD5Y, and these data suggest that a further refinement of the PES may be needed.

Acknowledgment. We are grateful to Dr. Ken Anderson of Southern Illinois University at Carbondale for analyzing the synthesized sample with a GC-mi-FTIR. K.B. acknowledges the National Science Foundation for supporting this research under CTS 0109053. Support for R.S.T. was provided under the auspices of the Office of Basic Energy Sciences, Division of Chemical Sciences, Geosciences, and Biosciences, U. S. Department of Energy, under contract number W-31-109-ENG-38.

Supporting Information Available: Tables of experimental data containing reaction conditions and species distributions. This material is available free of charge via the Internet at http://pubs.acs.org.

References and Notes

(1) Lindstedt, P. *Proc. Combust. Inst.* **1998**, *27*, 269.
(2) Richter, H.; Howard, J. B. *Prog. Energy Combust. Sci.* **2000**, *26*, 565.
(3) Miller, J. A. *Faraday Discuss.* **2001**, *119*, 461.
(4) Miller, J. A.; Klippenstein, S. J. *J. Phys. Chem. A* **2003**, *107*, 7783.
(5) Alkemade, U.; Homann, K. H. *Z. Phys. Chem.* **1989**, *161*, 19.
(6) Fahr, A.; Nayak, A. *Int. J. Chem. Kinet.* **2000**, *32*, 118.
(7) Scherer, S.; Just, T.; Frank, P. *Proc. Combust. Inst.* **2000**, *28*, 1511.
(8) Shafir, E. V; Slagle, I. R.; Knyazev, V. D. *J. Phys. Chem. A* **2003**, *107*, 8893.
(9) Howe, P. T.; Fahr, A. *J. Phys. Chem. A* **2003**, *107*, 9603.
(10) Anderson, K. B.; Tranter, R. S.; Tang, W.; Brezinsky, K.; Harding, L. B. *J. Phys. Chem. A* **2004**, *108*, 3403.
(11) Tranter, R. S.; Tang, W.; Anderson, K. B.; Brezinsky, K. *J. Phys. Chem. A* **2004**, *108*, 3406.
(12) Tang, W.; Tranter, R. S.; Brezinsky, K. *J. Phys. Chem. A* **2005**, *109*, 6056.
(13) Morter, C. L.; Farhat, S. K.; Adamson, J. D.; Glass, G. P.; Curl, R. F. *J. Phys. Chem.* **1994**, *98*, 7029.
(14) Atkinson, D. B.; Hudgens, J. W. *J. Phys. Chem. A* **1999**, *103*, 4242.
(15) DeSain, J. D.; Taatjes, C. A. *J. Phys. Chem. A* **2003**, *107*, 4843.
(16) Giri, B. R.; Hippler, H.; Olzmann, M.; Unterreiner, A. N. *Phys. Chem. Chem. Phys.* **2003**, *5*, 4641.
(17) Fernandes, R. X.; Hippler, H.; Olzmann, M. *Proc. Combust. Inst.* **2005**, *30*, 1033.
(18) Stein, S. E.; Walker, J. A.; Suryan, M.; Fahr, A. *Proc. Combust. Inst.* **1990**, *23*, 85.
(19) Kislov, V. V.; Nguyen, T. L.; Mebel, A. M.; Lin, S. H.; Smith, S. C. *J. Chem. Phys.* **2004**, *120*, 7008.
(20) Tang, W.; Tranter, R. S.; Brezinsky, K. *J. Phys. Chem. A*, **2006**, *110*, 2165.
(21) Tranter R. S.; Fulle D.; Brezinsky, K. *Rev. Sci. Instrum.* **2001**, *72*, 3046.
(22) Tranter, R. S.; Sivaramakrishnan, R.; Srinivasan, R.; Brezinsky, K. *Int. J. Chem. Kinet.* **2001**, *33*, 722.
(23) Tsang, W.; Lifshitz, A. *Annu. Rev. Phys. Chem.* **1990**, *41*, 559.
(24) Bhaskaran, K. A.; Roth, P. *Prog. Energy Combust. Sci.* **2002**, *28*, 151.
(25) Hopf, H. *Agnew. Chem., Int. Ed.* **1970**, *9*, 732.
(26) Hopf, H.; Bohm, I.; Kleinschroth, M. *J. Org. Synth.* **1981**, *60*, 41. Also at: *http://www.orgsyn.org/orgsyn/orgsyn/prepContent.asp?prep=cv7p0485*, 2005.
(27) Seres, I.; Huhn, P. *Int. J. Chem. Kinet.* **1986**, *18*, 829.
(28) Hohlein, G.; Freeman, G. R. *J. Am. Chem. Soc.* **1970**, *88*, 4326.
(29) Hopf, H. *Chem. Ber.* **1971**, *104*, 1499.
(30) Holbrook, Piling, M. J.; Robertson, S. H. Unimolecular Reactions, 2nd ed.; John Wiley & Sons: New York, 1996.
(31) Troe, J. *J. Chem. Phys.* **1977**, *66*, 4745.
(32) Troe, J. *J. Chem. Phys.* **1977**, *66*, 4758.
(33) Kiefer, J. H. private communication.
(34) Li, S.; Petzold, L. R. *J. Comp. Appl. Math.* **2000**, *125*, 131.